PNL-4001-4
UC-90g

Development of Material for Open-Cycle MHD

Quarterly Report for the Period Ending June 1983

D. D. Marchant
J. L. Bates

November 1983

Prepared for the U.S. Department of Energy
under Contract DE-AC06-76RLO 1830

Pacific Northwest Laboratory
Operated for the U.S. Department of Energy
by Battelle Memorial Institute

Battelle

PNL-4001-4

DISCLAIMER

PACIFIC NORTHWEST LABORATORY
operated by
BATTELLE
for the
UNITED STATES DEPARTMENT OF ENERGY
under Contract DE-AC06-76RLO 1830

Printed in the United States of America
Available from
National Technical Information Service
United States Department of Commerce
5285 Port Royal Road
Springfield, Virginia 22161

NTIS Price Codes
Microfiche A01

Printed Copy

Pages	Price Codes
001-025	A02
026-050	A03
051-075	A04
076-100	A05
101-125	A06
126-150	A07
151-175	A08
176-200	A09
201-225	A010
226-250	A011
251-275	A012
276-300	A013

PNL-4001-4
UC-90g

DEVELOPMENT OF MATERIALS FOR OPEN-CYCLE MHD

Quarterly Report for the Period
Ending June 1983

D. D. Marchant
J. L. Bates

November 1983

Prepared for
the U.S. Department of Energy
under Contract DE-AC06-76RLO 1830

Pacific Northwest Laboratory
Richland, Washington 99352

SUMMARY

Pacific Northwest Laboratory (PNL) is conducting an ongoing study of channel components for open-cycle, coal-fired magnetohydrodynamic (MHD) generators. Specifically, electrodes and insulators are being developed. The electrical conductivity has been measured on several compositions based on hafnium oxide, rare earth oxides, and indium oxide and on In_2O_3-SnO_2 compositions. Indium oxide at present appears to be the main constituent required for high conductivity. In the indium oxide-rare earth oxides-hafnium oxide compositions, the indium forms compounds with the other elements and is present in samples as individual grains and not as a contaminant along the grain boundary. In the In_2O_3-SnO_2 compositions, adding SnO_2 to In_2O_3 produces compositions with higher conductivity than pure In_2O_3.

CONTENTS

FIGURES

TABLES

INTRODUCTION

Pacific Northwest Laboratory (PNL)[a] is developing and testing ceramic electrodes and insulators and other channel components for open-cycle, coal-fired magnetohydrodynamic (MHD) generators as part of the U.S. Department of Energy's (DOE) Power Generation Program. The PNL program is divided into four tasks:

- development and fabrication of electrodes/insulators
- design and testing of electrodes/insulators
- characterization and evaluation of electrode/insulator materials
- measurement of thermal, electrical, and mechanical properties.

The objectives of the PNL program are to develop:

- electrodes that can withstand the severe corrosive and erosive environment of an MHD channel and that will transfer electrical current efficiently during long channel operation
- insulators that can withstand the corrosive and erosive environment and maintain adequate electrical resistivity during long channel operation
- electrode and insulator designs that are compatible with the demands of channel assembly, operation, and disassembly.

Because the tasks are interrelated, the quarterly reports for this program are organized by activities and not necessarily by specific tasks. This report summarizes measurement of the electrical conductivity of several ceramic compositions.

(a) Operated for DOE by Battelle Memorial Institute.

TECHNICAL PROGRESS

Adding indium oxide (In_2O_3) to rare earth oxides-hafnium oxide compositions has resulted in increased electrical conductivity, especially at temperatures between room temperature and 1300K. Tin oxide (SnO_2) additions also increase electrical conductivity, but the increase is not as great as with In_2O_3. Because SnO_2 appears to be more corrosion resistant than In_2O_3 (Marchant and Bates 1983b, pp. 3-7), conductive ceramics containing SnO_2 for increased corrosion resistance and In_2O_3 for increased electrical conductivity are being developed. This quarterly report emphasizes work that has been conducted on electrical conductivity.

ELECTRICAL CONDUCTIVITY

The electrical conductivity of two types of compositions is discussed in this report. The first group consists of a series of rare earth oxides-hafnium oxide compositions containing In_2O_3 additions. Phase analysis work is included to better understand the conductivity data. The second group consists of In_2O_3-SnO_2 compositions at different ratios to determine the ratio that yields the greatest conductivity. This ratio will then be added to the rare earth oxides-hafnium oxide compositions.

Indium Oxide-Rare Earth Oxides-Hafnium Oxide Compositions

The electrical conductivities of seven samples were measured using methods described by Marchant and Bates (1983a). The Marchant and Bates report also includes some preliminary conductivity data on some of the seven samples. This quarterly report includes more experimental data and a more complete analysis of all the data.

Conductivity as a function of temperature for the seven samples is shown in Figure 1. The legend on the figure indicates the indium oxide content for each sample and shows the two compositions that contain more praseodymium oxide than the others.

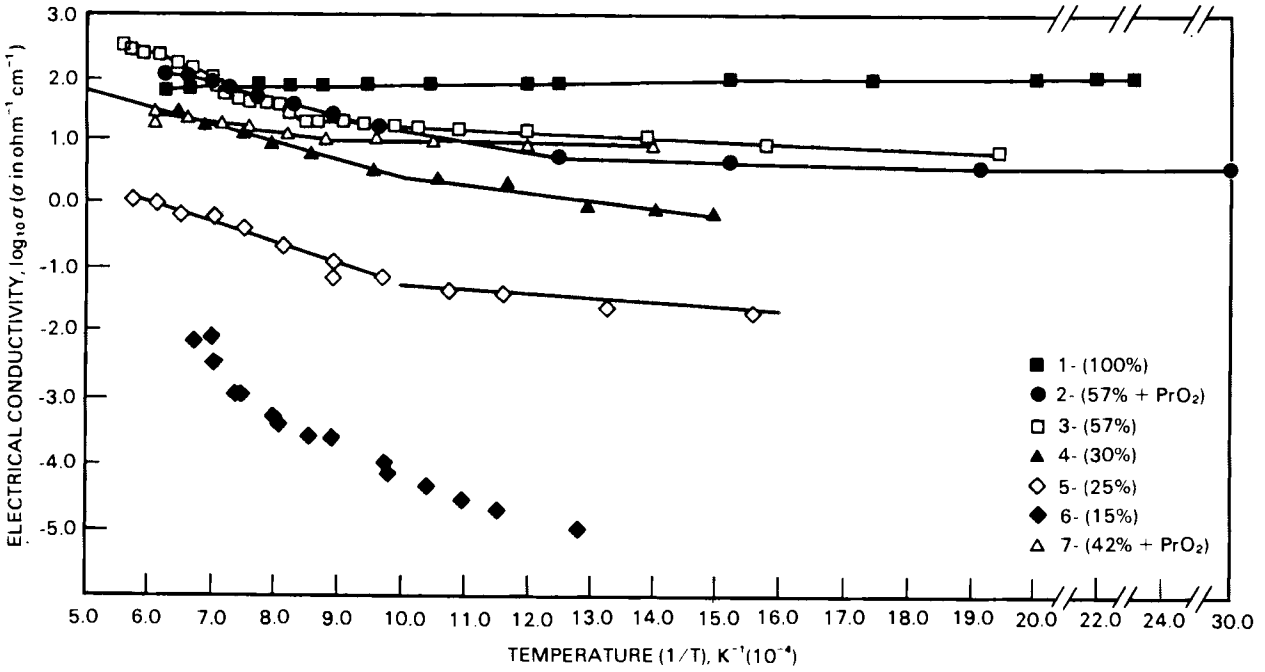

FIGURE 1. Electrical Conductivity as a Function of Temperature for Several Rare Earth Oxides-Hafnium Oxide Compositions Containing Indium Oxide. The solid lines represent the least squares fit to the data.

The composition of each sample in Figure 1 is given in Table 1. These compositions are based on analysis using the scanning electron microscope with energy dispersive x-ray analysis (SEM/EDX). The equations used to generate the lines representing the least squares fit to the data (Figure 1), the activation energy used to describe the temperature dependence of the conductivity, and the temperature range for both the least squares fit and the activation energy are also included in Table 1. In the chemical formulations, the nonstoichiometric praseodymium oxide is represented as PrO_2, although the starting powder prior to coprecipitation was Pr_6O_{11}. This representation is the common method of labeling praseodymium oxide.

For these seven compositions, the electrical conductivity increased with increasing In_2O_3 content. The low-temperature activation energies tended to decrease with increasing In_2O_3 content. The activation energy for In_2O_3 was a

TABLE 1. Composition of Samples Shown in Figure 1

Sample No.	Composition, mol%	Electrical Conductivity,[a] $ohm^{-1}cm^{-1}$ A	Electrical Conductivity,[a] $ohm^{-1}cm^{-1}$ B	Activation Energy, eV	Temperature, K	Sample Designation
1	In_2O_3	1.752	-1.560×10^2	-0.03	397 to 1631	13-3
2	0.57 In_2O_3·0.43( )[b]	1.138	2.544×10^2	0.05	335 to 930	AO
		3.878	2.783×10^3	0.55	987 to 1647	
3	0.57 In_2O_3·0.43[ ][c]	1.660	4.425×10^2	0.09	513 to 1010	AB
		4.664	3.846×10^3	0.76	1781 to 1064	
4	0.30 In_2O_3·0.70[ ]	3.471	1.123×10^3	0.22	851 to 1052	LLL
		5.530	3.325×10^3	0.66	1052 to 1551	
5	0.25 In_2O_3·0.75[ ]	0.447	8.118×10^2	0.16	645 to 933	AG
		1.958	3.177×10^3	0.63	1031 to 1727	
6	0.15 In_2O_3·0.85[ ]	(d)	(d)	(d)	(d)	AF
7	0.42 In_2O_3·0.68( )	(e)	(e)	(e)	525 to 1105	AS
		2.177	1.328×10^3	0.26	1135 to 1688	

(a) $Log_{10}\ \sigma = A - BT^{-1}$ where T is in Kelvin.
(b) ( ) = (35.6 mol% PrO_2·6.0 mol% Yb_2O_3·58.4 mol% HfO_2).
(c) [ ] = [28.5 mol% PrO_2·4.8 mol% Yb_2O_3·66.7 mol% HfO_2].
(d) Not linear.
(e) Nearly temperature independent.

negative value, indicating a small increase in conductivity as the temperature decreased. One sample did not follow the general trend; Sample 7, which contained 42 mol% In_2O_3, had a higher conductivity than expected.

The seven samples were examined with x-ray diffraction (XRD). The results are given in Table 2, which also includes the chemical analysis determined by SEM/EDX. The higher electrical conductivity appears to be associated with the development of a body-centered-cubic (BCC) phase containing a high concentration of indium oxide. Pure In_2O_3 also forms the BCC crystal structure. The microstructures of the samples in Table 2 consisted of intermixed granular-shaped phases. No microstructures were found with the matrix phase surrounded by the second phase along the grain boundaries. Since the phases were examined at room temperature, the shapes of the phases at higher temperatures are not known. Large grains at room temperature generally imply that the phases will remain granular at higher temperatures.

The grain boundaries were further investigated using the transmission electron microscope (TEM). Sample 4 (0.30 In_2O_3) was first thinned to a thickness of 50 μm using mechanical grinding and then thinned by ion milling until a hole formed in the sample. The grains around the hole were examined using the TEM; the results are shown in Figures 2 and 3.

Analysis of the grains using the EDX spectrometer with the TEM identified three compositions. The compositions listed in the figures are nominal and represent the average of several measurements on several grains. Higher concentrations of In_2O_3 were not found along the grain boundaries, although In_2O_3 was found in individual grains. A pyrochlore phase was found by electron diffraction with the TEM; this phase was not identified by XRD because it was less than 10% of the total. Face-centered-cubic (FCC) and BCC phases were dominant.

The electrical conductivity increased due to formation of the BCC In_2O_3-type phase; the amount of BCC phase increases with increased In_2O_3 content. Attempts will be made to modify this phase by adding SnO_2 to In_2O_3.

Indium Oxide-Tin Oxide Compositions

As reported in Marchant and Bates (1983b), the rare earth oxides-hafnium oxide compositions that contained SnO_2 tended to be more corrosion resistant in

TABLE 2. Results of XRD and SEM/EDX Analyses for Six Compositions (see Figure 1)

Sample No.	Composition, mol%	XRD Relative Amount	SEM/EDX, mol% In_2O_3	PrO_2	Yb_2O_3	HfO_2
2	0.57 In_2O_3·0.43( )	Major BCC[(b)] In_2O_3-type structure; a_o = 10.130 Å[(c)]	79	7	2	12
		Minor FCC fluorite HfO_2-type structure; a_o = 5.18 Å[(d)]	9	32	4	55
3	0.57 In_2O_3·0.43[ ]	Major BCC In_2O_3-type structure; a_o = 10.14 Å	93	0	1	6
		Minor FCC fluorite HfO_2-type structure; a_o = 5.18 Å	28	2	3	67
4	0.30 In_2O_3·0.70[ ]	Equal BCC In_2O_3-type structure; a_o = 10.135 Å	52	14	3	31
		Equal FCC fluorite HfO_2-type structure; a_o = 5.15 Å	24	19	4	53
5	0.25 In_2O_3·0.75[ ]	Major FCC fluorite HfO_2-type structure; a_o = 5.175 Å	19	19	5	57
		Minor FCC fluorite PrO_2-type structure; a_o = 5.328 Å	30	23	3	44
		Minor BCC In_2O_3-type structure; a_o = 10.13 Å	(e)	(e)	(e)	(e)
6	0.15 In_2O_3·0.85[ ]	Major FCC fluorite HfO_2-type structure; a_o = 5.17 Å	11	28	5	56
		Minor BCC In_2O_3-type structure; a_o = 10.2 Å	74	3	15	8

(a) See Table 1 for nomenclature identification.
(b) BCC = body-centered cubic
FCC = face-centered cubic.
(c) Pure In_2O_3; a_o = 10.118 Å.
(d) Pure HfO_2; a_o = 5.10 Å.
(e) Not available.

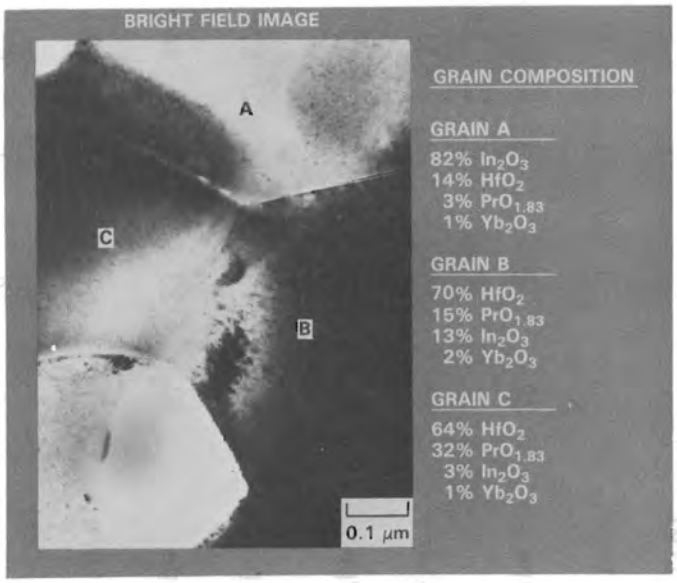

Microstructure and Microchemistry of Sample 4 from Table 1

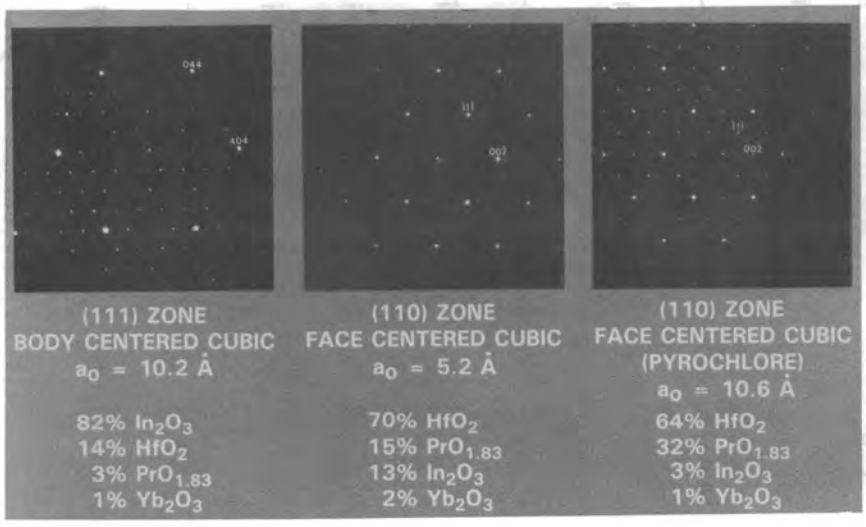

FIGURE 3. Crystal Structure Determined by Electron Diffraction of Sample 4 (see Table 1)

coal slag than those containing In_2O_3. Attempts to fabricate dense rare earth oxides-hafnium oxide compositions with only SnO_2 additions have not been successful. In addition, SnO_2 additions do not increase the electrical conductivity as much as In_2O_3 additions. Consequently, mixtures of In_2O_3-SnO_2 are being studied as additives. A brief study was conducted to determine which In_2O_2-SnO_2 mixture would yield the best electrical conductivity.

The electrical conductivities of several In_2O_3-SnO_2 compositions were measured as a function of In_2O_3 content (from 7 to 54 mol%). The samples were prepared by mixing powders.[a,b] All the starting powders had particle sizes less than -200 mesh (all sieve sizes are based on U.S. standard™).[c] Prior to mixing, the powders were prepared as slurries using ethanol; the slurries were placed in a polyethylene jar, mixed on the Spex mixer,[d] and then dried and pushed through a -14 mesh sieve. The powders were preslugged into a bar at 2.8×10^7 Pa (4000 psi), and the preslugged bar was pulverized through a -14 mesh sieve. The powders were cold die pressed into a bar at 3.5×10^7 Pa (5000 psi) and isostatically pressed at 18.6×10^7 Pa (27,000 psi). The powders were sintered in an air atmosphere at 1873K for 10 h, and samples were cut from the sintered bar using a diamond saw. The samples were bars about 2.5 cm long with an ~0.3-cm square cross section. The electrical conductivity was measured in an air atmosphere using the procedures previously described by Marchant and Bates (1983b).

The electrical conductivity results are shown in Figure 4. The electrical conductivity increased with increases in In_2O_3 content. The highest conductivity measured was for the 54 mol% In_2O_3. The curves drawn through the data points are described by the equations listed in Table 3. The activation energy used to describe the temperature dependence of the conductivity is also given in the table. The activation energy of the lower temperature portion of the

---

(a) Use of manufacturer names does not imply PNL endorsement.
(b) In_2O_3: 99.99% pure, D. F. Goldsmith Chemical and Metal Corp., Evanston, Illinois. SnO_2: 99.9% pure, Cerac, Inc., Milwaukee, Wisconsin.
(c) U.S.A. Standard Testing Sieve, Fisher Scientific Co., Seattle, Washington.
(d) Spex Industries, Inc., Metuchen, New Jersey.

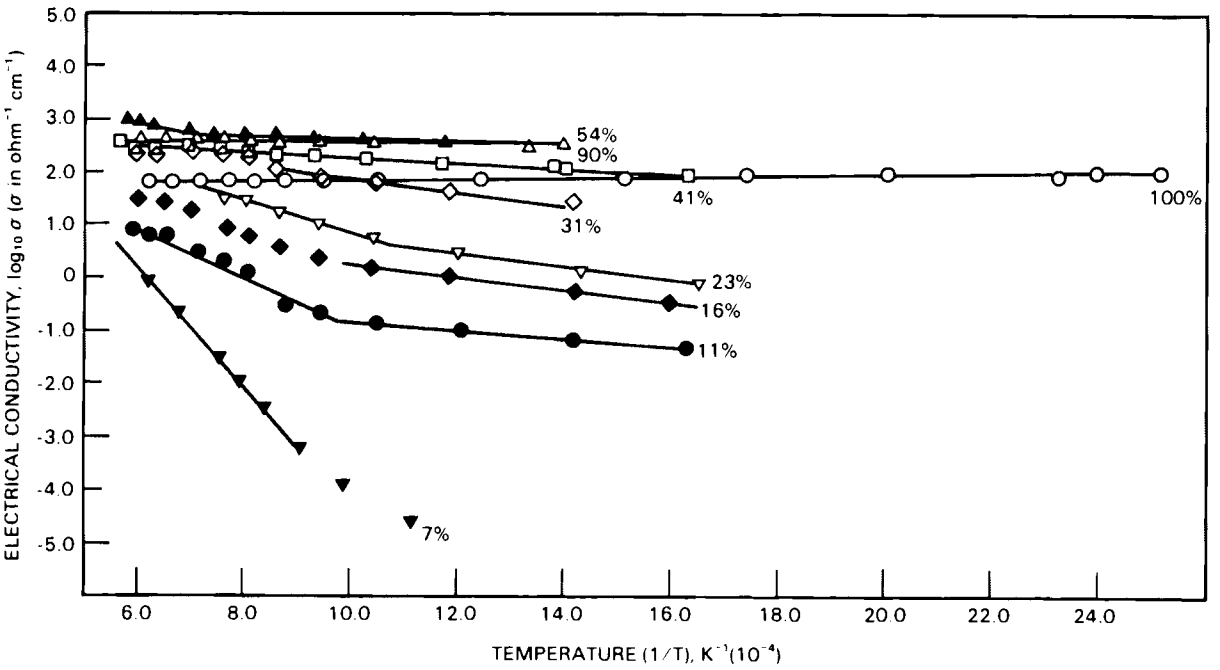

FIGURE 4. Electrical Conductivity as a Function of Temperature for Several In_2O_3-SnO_2 Compositions

electrical conductivity generally decreased with increasing In_2O_3 content. Pure In_2O_3, 90 mol% In_2O_3·10 mol% SnO_2, and 54 mol% In_2O_3·46 mol% SnO_2 have a low-temperature conductivity that is nearly independent of temperature.

Overview

One goal of this program is to develop ceramics with low temperature-dependent electrical conductivity. This dependence results in the reduction of current channeling in the ceramic when used as an electrode in an MHD channel. Current channeling occurs because the electric current passes through the electrode along the least resistive path. Temperature gradients are found in all three dimensions in the electrode due to the geometry of the electrode and the location of the water cooling. Consequently, a high-temperature dependence results in areas of the electrode having much greater electrical conductivities than other areas. Consequently, the current densities in the higher conducting areas may be much greater than the average, resulting in localized electrode damage. A low-temperature dependence of the conductivity results in a more uniform conductivity in the electrode and consequently in more uniform current distributions.

TABLE 3. Composition and Electrical Conductivity for Several In_2O_3-SnO_2 Materials

Composition, mol%		Electrical Conductivity,[a] $ohm^{-1}cm^{-1}$		Activation Energy, eV	Temperature, K	Sample Designation
In_2O_3	SnO_2	A	B			
7	93	(b)	(b)	(b)	(b)	FC-55
		6.814	11.090×10^3	2.20	1111 to 1726	
11	89	0.015	8.230×10^2	0.16	524 to 956	FC-56
		3.659	4.573×10^3	0.91	1060 to 1720	
16	84	1.409	1.155×10^3	0.23	606 to 961	FC-57
		(b)	(b)	(b)	(b)	
23	77	1.945	1.232×10^3	0.24	308 to 837	FC-58
		3.972	3.121×10^3	0.62	962 to 1433	
31	69	3.086	1.210×10^3	0.24	847 to 1148	FC-59
		(b)	(b)	(b)	(b)	
41	59	2.790	5.129×10^2	0.10	611 to 1738	FC-60
54	46	2.93	2.460×10^2	0.05	702 to 1342	FC-61
		3.98	1.672×10^3	0.33	1444 to 1725	
90	10	2.625	0.030	0.01	746 to 1720	FC-15-1
100	0	1.752	-1.551×10^2	-0.03[c]	401 to 1631	FC-13-3

(a) $\text{Log}_{10}\ \sigma = A - BT^{-1}$ where T is in Kelvin.
(b) Nonlinear.
(c) Nearly temperature independent.

Several other compositions are being measured to determine the range of compositions that will result in conductivities above those found for In_2O_3. The results of these measurements will be reported in the next quarterly. Since SnO_2 appears to be more corrosion resistant than In_2O_3, adding SnO_2 to the sample should also increase its corrosion resistance.

REFERENCES

Marchant, D. D., and J. L. Bates. 1983a. Development of Materials for Open-Cycle MHD - Quarterly Report for the Period Ending December 1982. PNL-4001-2, Pacific Northwest Laboratory, Richland, Washington.

Marchant, D. D., and J. L. Bates. 1983b. Development of Materials for Open-Cycle MHD - Quarterly Report for the Period Ending March 1983. PNL-4001-3, Pacific Northwest Laboratory, Richland, Washington.

DISTRIBUTION

No. of Copies

OFFSITE

M. Mintz
U.S. Department of Energy
Division of MHD
FE-26, F-338, GTN
Washington, DC 20545

M. Covington
DOE Butte Project Office
P.O. Box 3462
Butte, MT 59701

F. Herbaty, Sr., MHD
DOE Chicago Operations Office
9800 S. Cass Avenue
Argonne, IL 60639

T. Arrigoni
Technical Project Officer
PM-20, Mail Stop 920-215
Pittsburgh Energy Technology
U.S. Department of Energy
P.O. Box 10940
Pittsburgh, PA 15236

H. F. Chambers
Chief, MHD Management Section
PM-20, Mail Stop 920-215
Pittsburgh Energy Technology
U.S. Department of Energy
P.O. Box 10940
Pittsburgh, PA 15236

J. O. Hunze
DOE Operations Office
University of Tennessee Space Institute
Tullahoma, TN 37388

27 DOE Technical Information Center

No. of Copies

M. Petrick
Argonne National Laboratory
9700 S. Cass Avenue
Argonne, IL 60439

W. Redman
Argonne National Laboratory
9700 S. Cass Avenue
Argonne, IL 60439

Mr. Roepke PWT/PT
AEDC Division
Arnold Air Force Station, TN 37389

L. Whitehead, Calspan
AEDC Division
Arnold Air Force Station, TN 37389

R. V. Kessler
AVCO Everett Research Laboratory
2385 Revere Beach Parkway
Everett, MA 02149

F. Hals
AVCO Everett Research Laboratory
2385 Revere Beach Parkway
Everett, MA 02149

A. C. Dolbec
Advanced Fossil Power Systems
Electric Power Research Institute
P.O. Box 10412
Palo Alto, CA 94304

R. J. Ferraro
Electric Power Research Institute
P.O. Box 10412
Palo Alto, CA 94304

D. DeCoursin
FluiDyne Engineering Corp.
5900 Olson Memorial Highway
Minneapolis, MN 55422

No. of Copies

R. Rhodenizer
General Electric Corp.
Research Laboratories
Schenectady, NY 12305

J. C. Cutting
Gilbert Associates, Inc.
P.O. Box 1498
Reading, PA 19603

2 A. Dawson
Massachusetts Institute of Technology/PFC
NW-16-130
Cambridge, MA 02139

D. Murphee
Mississippi State University
Aerophysics and Aerospace Engineering
P.O. Drawer A/AP
Mississippi State, MS 39762

J. Orth
Montana Energy and MHD R&D Institute
P.O. Box 3890
Butte, MT 59701

G. E. Youngblood
Montana Energy and MHD R&D Institute
P.O. Box 3890
Butte, MT 59701

R. Rosa
Montana State University
Department of Mechanical Engineering
Bozeman, MT 59715

J. Sherick
Mountain States Energy, Inc.
P.O. Box 3767
Butte, MT 59701

No. of Copies

J. Winters
NASA/Lewis Research Center
21000 Brookpart Road
Cleveland, OH 44135

S. Demetriades
STD Corporation
P.O. Box C
Arcadia, CA 91006

C. Maxwell
STD Corporation
P.O. Box C
Arcadia, CA 91006

C. H. Kruger
Stanford University
Palo Alto, CA 94305

M. Bauer
TRW, INC.
One Space Park
Redondo Beach, CA 90278

J. Hardgrove
TRW, INC.
One Space Park
Redondo Beach, CA 90278

M. A. Scott
University of Tennessee Space Institute
Tullahoma, TN 37388

S. Wu, Director
University of Tennessee Space Institute
Tullahoma, TN 37388

A. Jones
Westinghouse Electric Corporation
Waste Technology Services Division
P.O. Box 10864
Pittsburgh, PA 15236

No. of
Copies

FOREIGN

R. P. Indwar
Central Mine Planning and
Design Institute, Ltd.
Gondwana Place
Kanke Rd.
Ranchi 834008 India

ONSITE

DOE Richland Operations Office

H. E. Ransom

No. of
Copies

23 Pacific Northwest Laboratory

J. L. Bates (2)
S. K. Edler
C. R. Hann
P. E. Hart
D. D. Marchant (10)
R. P. Turcotte
Technical Information (5)
Publishing Coordination (2)